EPJ B
Condensed Matter and Complex Systems
EPJ.org your physics journal

Eur. Phys. J. B (2019) 92: 13 DOI: 10.1140/epjb/e2018-90280-8

Nickel oxide/cobalt phthalocyanine nanocomposite for potential electronics applications

Parambil Abdul Lathief Sheena, Aikkara Sreedevi, Chandra Viji, and Varghese Thomas

edp sciences
Società Italiana di Fisica
Springer

Eur. Phys. J. B (2019) 92: 13
https://doi.org/10.1140/epjb/e2018-90280-8

THE EUROPEAN PHYSICAL JOURNAL B

Regular Article

Nickel oxide/cobalt phthalocyanine nanocomposite for potential electronics applications

Parambil Abdul Lathief Sheena[1,2,3], Aikkara Sreedevi[4], Chandra Viji[5], and Varghese Thomas[3,a]

[1] Department of Physics, M.E.S. Asmabi College, P. Vemballur 680671, Kerala, India
[2] Department of Physics, Newman College, Thodupuzha 685584, Kerala, India
[3] Nanoscience research centre (NSRC), Department of Physics, Nirmala College, Muvattupuzha 686661, Kerala, India
[4] Department of Applied Science and Humanities, Thejus Engineering College, Thrissur 680584, Kerala, India
[5] Department of Physics, Maharajas College, Ernakulam, Kerala 682011, Kerala, India

Received 23 April 2018 / Received in final form 30 September 2018
Published online 16 January 2019

Abstract. The effect of cobalt phthalocyanine on the dielectric behaviour and ac conductivity of nickel oxide nanoparticles is reported in this study. Solvent evaporation method is employed for the synthesis of nickel oxide/cobalt phthalocyanine (NiO–CoPc) nanocomposite. The structure and morphology of the synthesized nanocomposites are analysed using XRD and TEM. Dielectric properties and ac conductivity of NiO/CoPc sample is estimated as a function of frequency at different temperatures. The study reveals that the dispersion is due to interfacial polarization of Maxwell–Wagner type. The loss tangent in the low frequency region can be considerably reduced with the incorporation of CoPc. The presence of two semicircular arcs in the Cole–Cole plot points out the existence of grain and grain boundary conduction in the nanocomposite sample. High permittivity together with good thermal stability makes NiO/CoPc nanocomposite a potential candidate for applications in molecular electronics.

1 Introduction

Nanodielectric materials have attracted much attention because of their potential applications in power electronics industry. The need for miniaturization of electronic components triggered the search for new materials with high dielectric constant and low dielectric loss [1]. Organic/inorganic nanocomposites are of widespread interest due to their use in various electronic and photonic devices. Metal phthalocyanines are a class of organic semiconductors with good thermal and chemical stability [2]. Their unique optical and electrical properties make them eligible candidates in electrochemical sensors, photovoltaic devices and photodetectors [3–5]. Dielectric materials with high permittivity and good thermal stability have a key role in microelectronics. Transition metal oxides are one among the high-k materials with best resistive switching property. These excellent features make the organic/inorganic nanocomposites applicable in various fields like molecular electronics, catalysis and optoelectronic devices.

The present work reports the electrical properties of NiO/CoPc nanocomposite as a function of frequency and temperature. The studies on the effect of frequency in the dielectric behaviour and ac conductivity give valuable information about the conduction phenomena in the material. Stoichiometric NiO with very low conductivity at ordinary temperatures is classified as a Mott-Hubbard insulator. The increase in the number of Ni^{2+} vacancies (defects) in the sample can enhance its conductivity [6]. CoPc possessing extended conjugated structure exhibits good electrical conductivity [3]. Hence, the introduction of CoPc into the NiO lattice can tune the properties of NiO, thereby making the composite a promising material for electronic and optoelectronic applications. To date, there are no reports on the electrical studies of NiO/CoPc nanocomposite.

2 Experimental details

2.1 Materials

Nickel nitrate hexahydrate ($Ni(NO_3)_2{\cdot}6H_2O$, 99.8%, Merck), ammonium carbonate ($(NH_4)_2CO_3$, 99.9%, Merck), cobalt phthalocyanine (CoPc, Sigma Aldrich), dimethyl formamide, dimethyl sulphoxide and ethanol (Merck) are used for the synthesis of the nanocomposite.

[a] e-mail: ptvarghese07@yahoo.co.in

2.2 Synthesis of NiO–CoPc nanocomposite

The NiO–CoPc nanocomposite with two different weight percentages of CoPc is prepared by solvent evaporation method. Cobalt phthalocyanine (1 wt.% and 2 wt.%) is dissolved in a solvent mixture containing 50% dimethyl sulphoxide, 30% dimethyl formamide and 20% ethanol under magnetic stirring and simultaneous heating at 60 °C. NiO nanoparticles prepared by chemical precipitation method and calcined at 500 °C are gradually added to this solution [7]. The material obtained after complete evaporation of the solvent mixture is washed several times and dried at 100 °C in a hot air oven for 18 h to get the nanocomposite. The synthesized NiO nanoparticles and the NiO/CoPc nanocomposites with 1 wt.% and 2 wt.% CoPc are denoted as S0, S1 and S2, respectively.

2.3 Characterization

The structural analysis of the samples are done by X-ray powder diffraction method using Bruker D8 advance X-ray diffractometer (λ = 1.5406 Å, step size = 0.020° and step time = 32.8 s) with CuKα radiation (λ = 1.5406 Å, X-ray tube voltage = 40 kV and current = 35 mA) from 0 to 90 °C. Transmission electron microscopy images are recorded on a Jeol/JEM 2100 instrument at an accelerating voltage of 200 kV. For electrical measurements, NiO and NiO/CoPc nanocomposite samples are consolidated into pellets with diameter 13 mm and thickness 1.5 mm at a pressure of about 7 GPa using a hydraulic press. The pellets prepared are then sintered at 300 °C for 2 h. For good electrical contact, both faces of the pellets are coated with silver paste.

Dielectric measurements are done in the frequency range of 50 Hz–50 MHz at selected temperatures in the range 300–363 K using impedance analyser (Wayne Kerr H-6500B model). The complex dielectric constant is represented by

$$\varepsilon = \varepsilon' - j\varepsilon'',$$

where ε' is the real part of dielectric constant which defines stored energy and ε'' is the imaginary part which represents dissipated energy within the medium [8]. The principle of parallel plate capacitor is employed for the calculation of dielectric constant. The capacitance of a parallel plate capacitor is given by

$$C = \varepsilon_0 \varepsilon' A/d,$$

where A and d are the face area and thickness of the pellet respectively, ε_0 the permittivity of free space and ε' the dielectric constant of the given sample. The dielectric constant ε' is given by

$$\varepsilon' = Cd/\varepsilon_0 A.$$

The AC conductivity of the sample (σ_{ac}) is given as

$$\sigma_{ac} = 2\pi f \varepsilon_0 \varepsilon' \tan\delta,$$

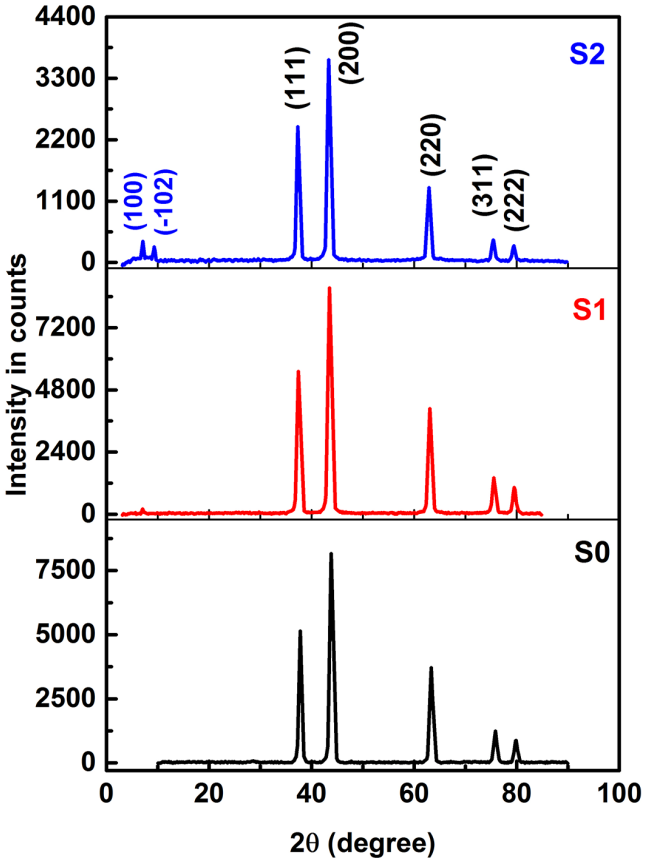

Fig. 1. XRD spectra of NiO and NiO/CoPc nanocomposites.

where f is the applied electric field frequency and tan δ the loss tangent.

3 Results and discussion

3.1 XRD analysis

The X-ray diffraction patterns of S0, S1 and S2 samples are shown in Figure 1. All the diffraction peaks are sharp, indicating the crystallinity of the sample. The 2θ values revealed the formation of face centred cubic phase of NiO (JCPDS Card 73-1519) which can be indexed as (111), (200), (220), (311) and (222) planes. The diffraction pattern of S2 contains two additional peaks at 7.085° and 9.307° which confirm the formation of NiO/CoPc nanocomposite. These peaks correspond to (100) and ($\bar{1}02$) planes of β CoPc, respectively [9]. The peaks of CoPc are not observed in the diffraction pattern of S1, which may be due to its lower concentration. The crystallite size of samples are obtained from the line broadening of the diffraction peaks using Scherrer equation, $D = k\lambda/\beta\cos\theta$ [10]. Average crystallite size calculated for the S0, S1 and S2 samples are 16, 17.5 and 18 nm, respectively.

3.2 TEM analysis

In order to reveal the morphology and size of the synthesized particles, TEM images of pure and nanocomposite

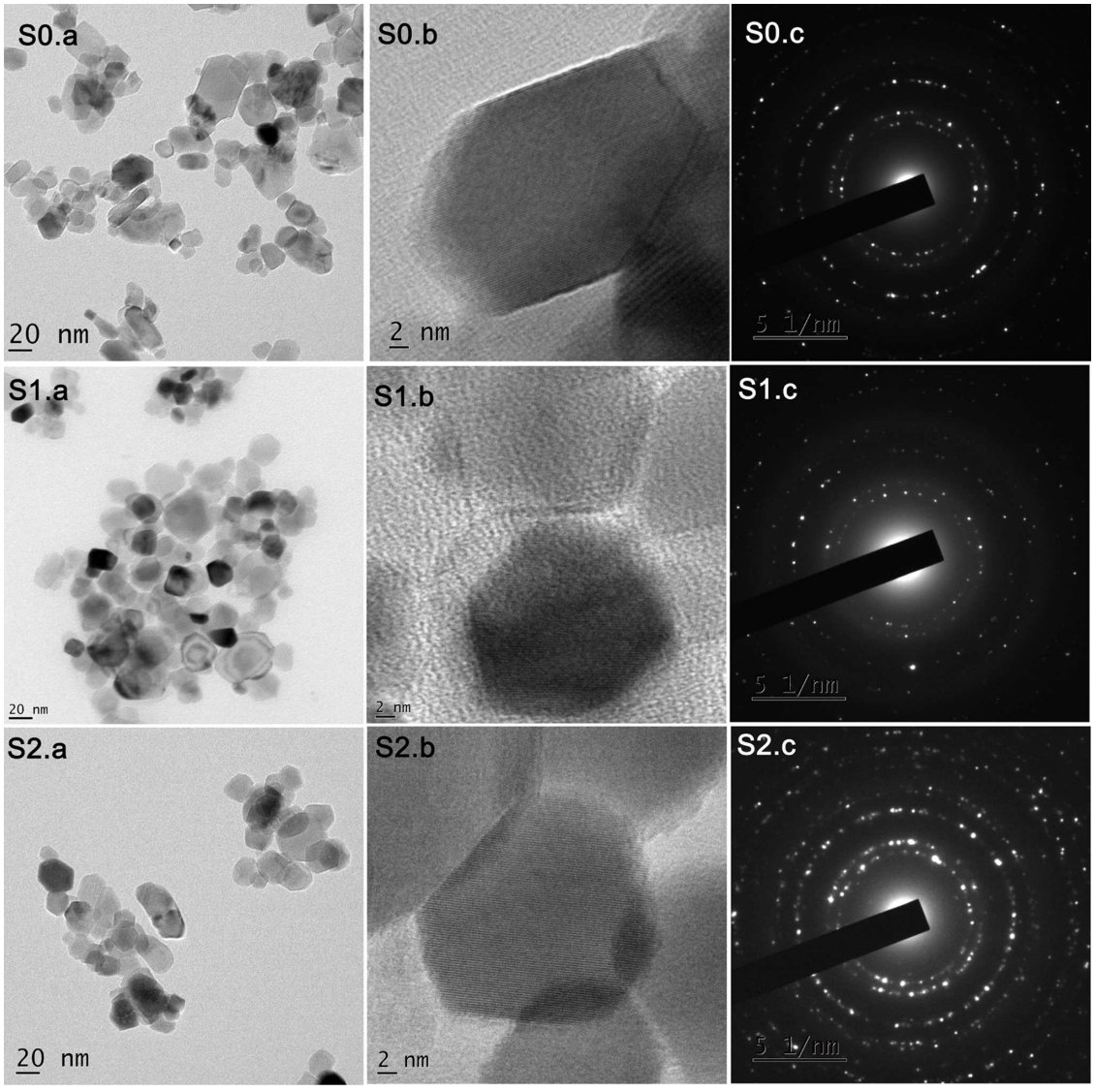

Fig. 2. TEM images of NiO (S0) and NiO/CoPc nanocomposites (S1 and S2).

samples are recorded as displayed in Figure 2. Well dispersed non-spherical particles are clearly seen in the bright field image. HRTEM images show fringe pattern for all the samples. SAED patterns of all samples show clear spots arranged in ring shape corresponding to different planes of NiO. The histogram showing the particle size distributions of the samples are plotted in Figure 3. The average particle size obtained from TEM images for the samples S0, S1 and S2 are 21, 23.1 and 23.9 nm, respectively.

3.3 Dielectric properties

Dielectric response of NiO/CoPc nanocomposites is examined in the frequency range of 50 Hz–5 MHz. The frequency dependence of dielectric constant (ε), loss tangent (tan δ) and AC conductivity (σ_{ac}) at selected temperatures for the NiO/CoPc nanocomposite samples are studied.

The variation in the real part of dielectric constant (ε') with frequency of the samples for different temperatures is plotted in Figure 4. The values of ε' and tan δ at 303 K for the three samples at selected frequencies are shown in Table 1. The ε' has very high value in the low-frequency region, which decreases rapidly with increase in frequency and becomes almost constant at higher frequencies for all temperatures.

The dielectric behaviour of nanostructured materials depends on the excitation of bound electrons, lattice vibrations, dipole orientation and space-charge polarization [11]. The dielectric dispersion curve can be described using Koop's theory [12], which is based on the Maxwell–Wagner model [13]. According to this model, the dielectric structure is composed of grains which are highly conducting, separated by relatively poor conducting regions called grain boundaries. Under the influence of electric field, localized accumulation of charges occur at the

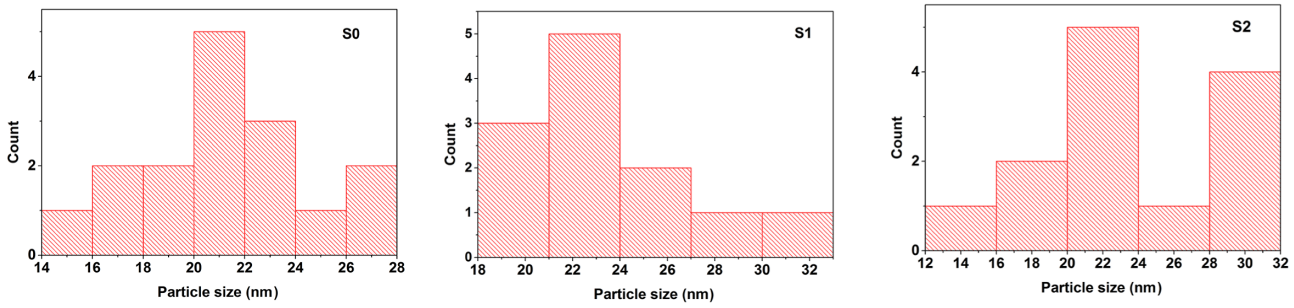

Fig. 3. Histogram of samples S0, S1 and S2.

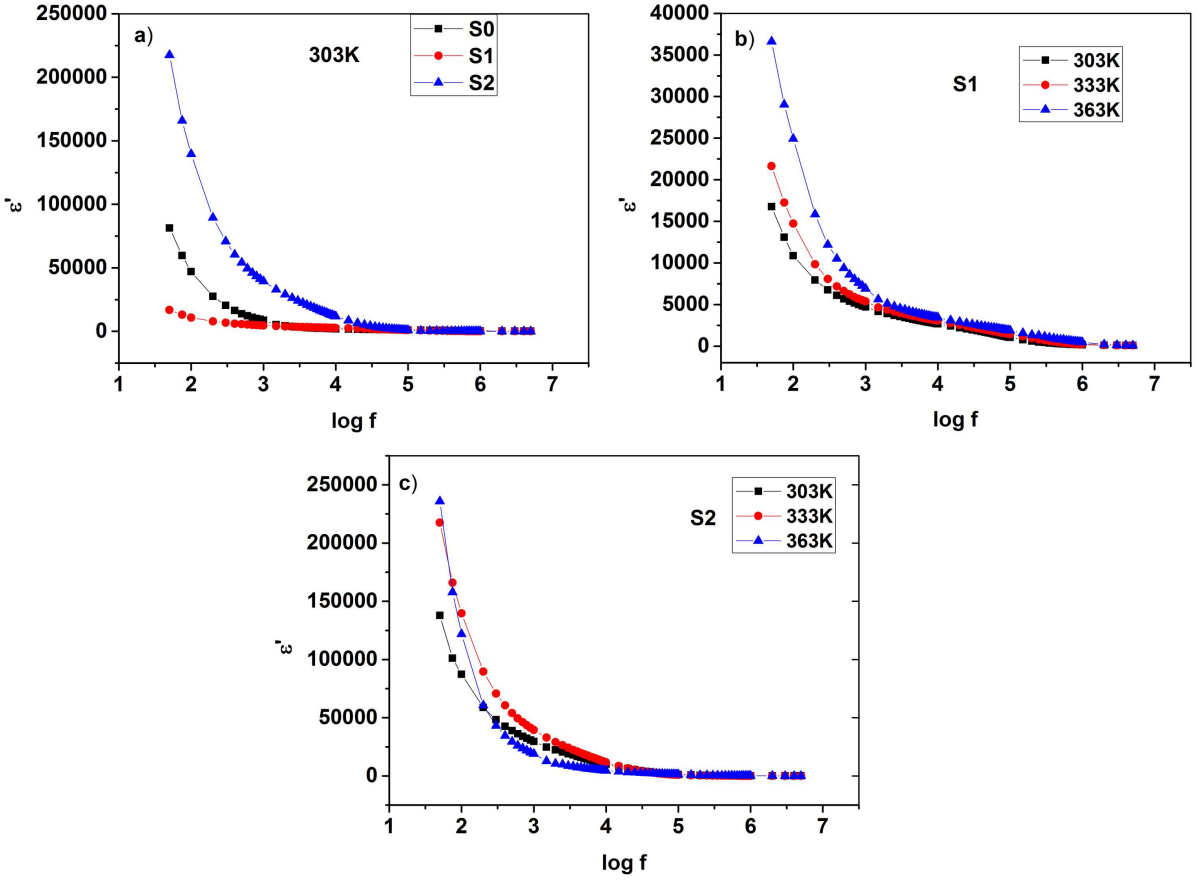

Fig. 4. Variation of dielectric constant with frequency and temperature; (a) comparison of S0, S1 and S2 samples at 303 K, (b) S1 and (c) S2 at various temperatures.

grain boundaries which results in interfacial/space charge polarization.

As reported in the literature, the conduction process in NiO is described by correlated barrier hopping model (CBH) [14,15]. CBH model suggests two types of carrier hopping in NiO: (i) inter-well hopping – the hopping of a hole from a Ni^{3+} ion located in one defect potential well to a Ni^{2+} or O_2- ion in an adjacent defect potential well and (ii) intra-well hopping – the hopping of holes between ions within one defect potential well. These holes on reaching the grain boundary get piled up due to its high resistivity, thereby producing space charge polarization. The enhanced dielectric constant at low frequency is due to the space-charge polarization caused by impurities or crystal defects. The decrease of dielectric constant at higher frequencies is due to the lagging of charge carriers contributing to polarization behind the applied field. At low frequencies, the temperature-dependent dipolar and space charge polarizations predominate. As temperature increases, the dipoles rotate more freely and increase the dipolar polarizability. With increased temperature, the space charge polarization density is sufficiently large at high temperatures, which further enhances the dielectric properties [16]. The addition of CoPc can cause alterations in the space charge distribution, which in turn varies the dielectric constant [17]. As the concentration of CoPc is

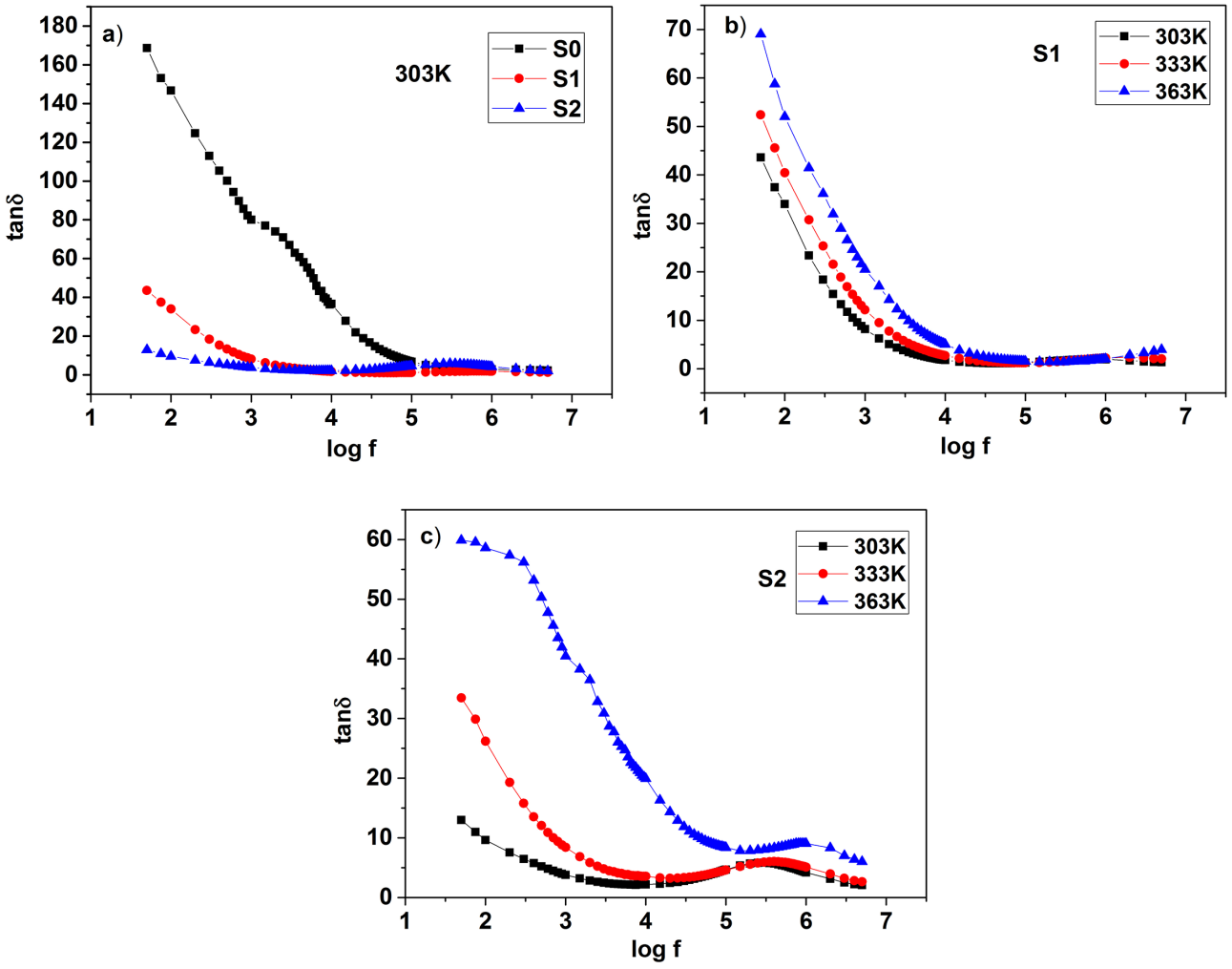

Fig. 5. Variation of loss tangent with frequency and temperature. (a) Comparison of S0, S1 and S2 samples at 303 K, (b) S1 and (c) S2 at various temperatures.

Table 1. Values of ε' and tan δ at 303 K for S0, S1 and S2.

Frequency	S0		S1		S2	
	ε'	tan δ	ε'	tan δ	ε'	tan δ
1 KHz	8727	80	4709	8.2	39522	3.8
10 KHz	1937	36.7	2672	1.79	11754	2.18
100 KHz	1116	6.75	1052	1.26	979	4.67

increased, the values of dielectric constants are elevated to higher values in the low-frequency regime. This may be due to the increase in internal stress, which can enhance the space charge polarization.

High dielectric constant (high-k) materials are used in semiconductor industry as gate oxide in metal oxide semiconductor field effect transistors (MOSFETs). The dielectric constants of NiO and NiO/CoPc nanocomposite samples are high compared to SiO_2, which has been used as the gate dielectric in MOSFETs. Scaling demanded drastic decrease of SiO_2 thickness to increase the gate capacitance, but failed because of high gate oxide leakage current. By replacing SiO_2 with other high dielectric constant materials, an enhanced gate capacitance can be achieved without leakage effects. Another remarkable property of high-k materials, called resistive switching (RS), is utilized for improving the performance of resistive random access memory (RRAM). Transition metal oxides are high-k materials with the best RS properties [18].

The dielectric loss (tan δ) as a function of frequency for different temperatures is shown in Figure 5. It decreases with increase in frequency and attains a constant value at high frequencies for all temperatures. In nanomaterials, the absorption current produced due to impurities, defects and space charge formation in the interphase layers results in a dielectric loss [19]. The absorption current and hence the dielectric loss gets reduced as the applied frequency increases. The plot of S2 displays the existence of a single relaxation peak in the high-frequency region. This may be attributed to the dipole moment of the defect pair formed from the oxygen vacancy and the central metal ion

Table 2. Equivalent circuit parameters of S0, S1 and S2 samples.

Sample	R_S (Ω)	CPE1(F)	$R1$(Ω)	$n1$	CPE2/C2(F)	$R2$ (Ω)	$n2$
S0	99	8.521E-08	341	0.6794	–	–	–
S1	146	3.43E-08	4243	0.7909	2.651E-10	304	0.989
S2	155	8.522E-7	1226	0.703	2.979E-10	212	–

of phthalocyanine. The peak intensity increases and shifts to high frequency side with increase in temperature. With increase in temperature, the oxygen vacancies are released from the defect centres, which causes an increase in peak intensity [20]. As seen from the figure, the dielectric loss is considerably reduced with increase in CoPc concentration. With the addition of CoPc, tan δ of NiO at 100 Hz reduced from 146 for S0 to 9.6 for S2. High dielectric constant and reasonably low dielectric loss are the basic characteristics of dielectric materials to be used as embedded capacitors for decoupling applications [21].

For a better understanding of the dielectric behaviour of the synthesized nanocomposites, complex impedance spectroscopic technique is employed. The grain and grain boundary contributions to the overall impedance can be resolved by fitting the experimental response to that of an equivalent circuit. The Cole-Cole plots of the samples at room temperature and the corresponding equivalent circuits (shown in the inset) fitted using EIS spectrum analyser are shown in Figure 6. The single semicircle detected for sample S0 (Fig. 6) indicates Maxwell–Wagner type of dielectric polarization arising at the grain boundary [22]. It can be seen that the curve is not a perfect semicircle, which indicates a non-uniform distribution of relaxation mechanisms. The data can be modelled with a circuit consisting of a resistance R_S in series with a parallel combination of a resistor $R1$ and a constant phase element (CPE). CPE1 takes into account the frequency dispersion of the capacitance values and the spatial inhomogeneity of the system [23]. The impedance of CPE is of the form $Z_Q = (j\omega) - n/Q$, where Q is a constant and n is the exponent with a value between $0 < n < 1$, n is a measure of the capacitive nature of the component [24]. Typical values of the parameters R_S, $R1$ and CPE1 obtained from the fits are given in Table 2.

In contrast to NiO, the Cole-Cole plot of NiO/CoPc nanocomposites exhibit two semicircles. The semicircular arc at high frequency represents the contribution of grains, and the arc in lower frequency is attributed to the grain boundary effects [25]. The bulk and grain boundary effects can be separated by fitting the experimental data with an equivalent circuit, which usually consists of two parallel RC circuits connected in series. The Cole-Cole plots and the fitted equivalent circuits of the samples S1 and S2 are shown in Figures 6b and 6c, respectively. The existence of two semicircular arcs suggests the electrical heterogeneous nature of the nanocomposite. Table 2 displays the values of resistances and capacitances obtained by fitting the impedance data of the nanocomposite samples. $R1$ and CPE1 describe the resistance and capacitance of the grain boundary, while $R2$ and CPE2 represent the resistance and capacitance of the conducting bulk material. The values show that the grain boundaries are more

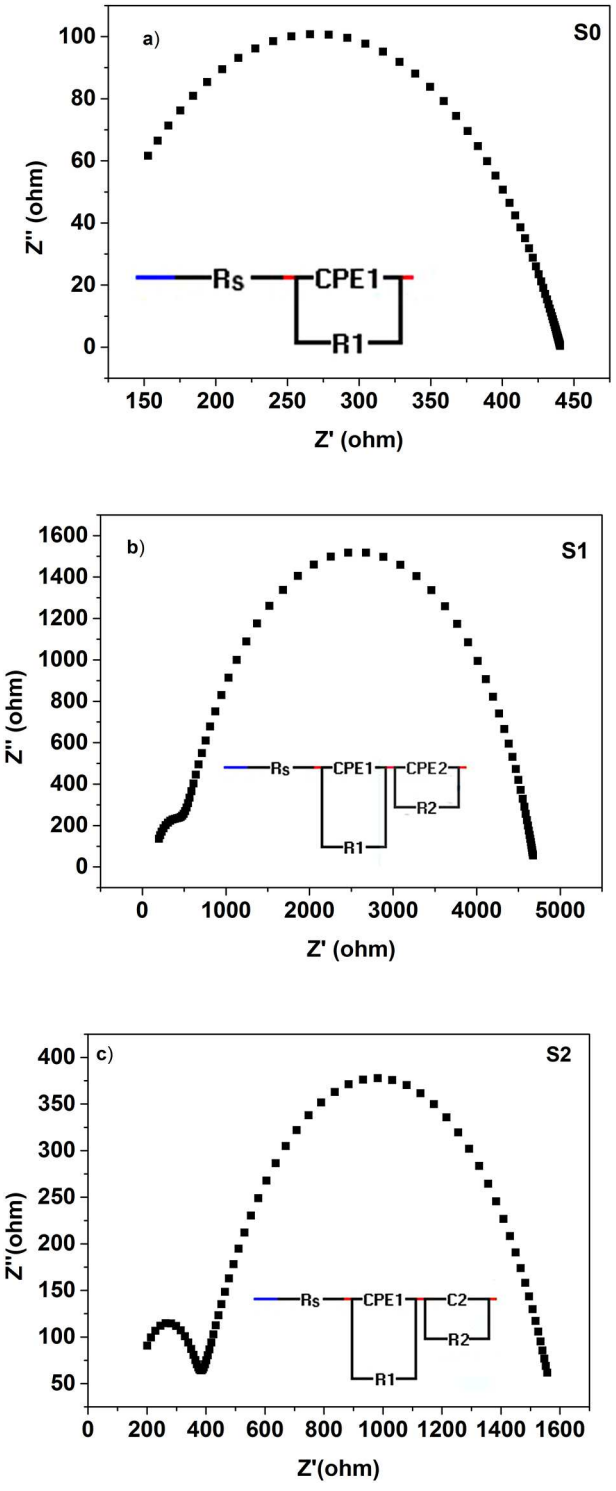

Fig. 6. Modulus plot of NiO and NiO/CoPc nanocomposites.

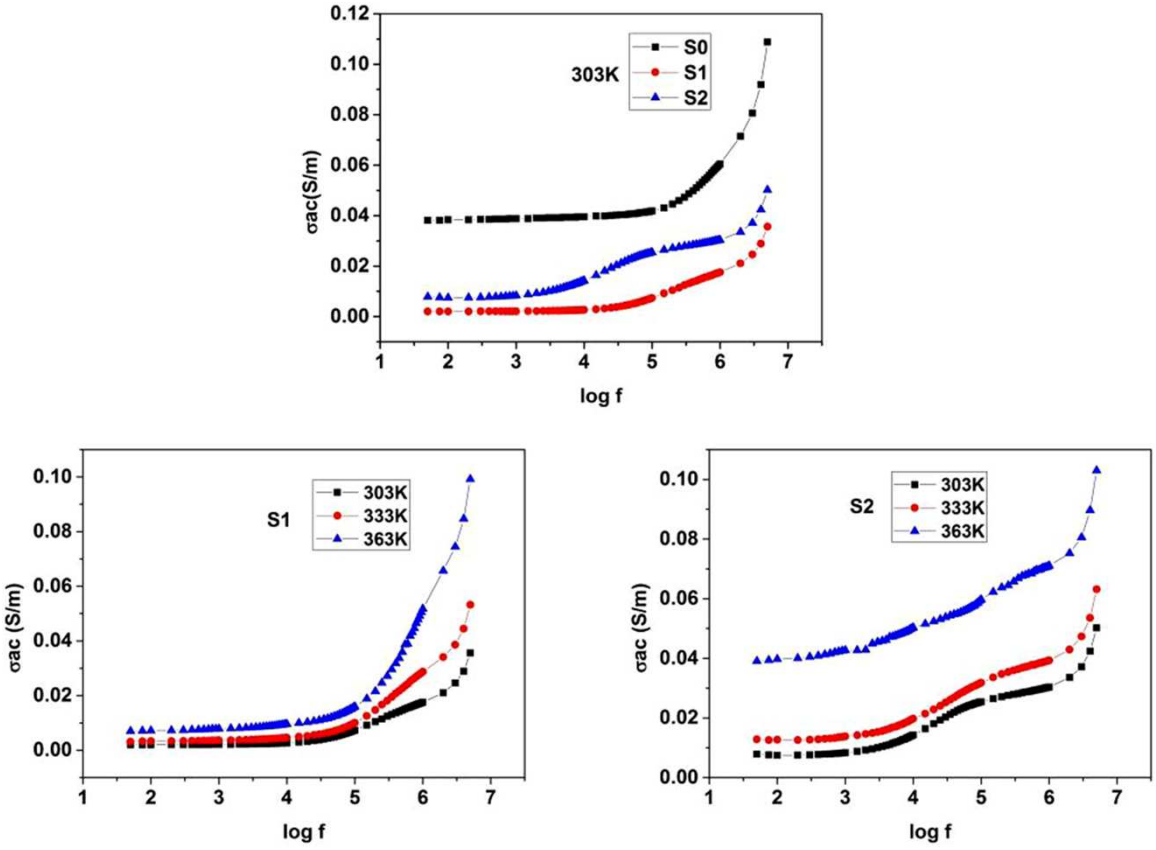

Fig. 7. Variation of σ_m(ac) with frequency of NiO and NiO/CoPc at 300 K and NiO/CoPc composites at different temperatures.

capacitive and resistive as compared to the grains in the sample.

3.4 AC conductivity

The variation of measured AC conductivity σ_{ac} as a function of frequency for selected temperatures is studied and is presented in Figure 7. At all temperatures, σ_{ac} is found to be more or less independent of the applied signal frequency up to about 10 kHz, while at higher frequencies, it increases with the applied frequency. In the low-frequency region, inter-well hopping, which is responsible for DC conduction, dominates intra-well hopping. Generally, the measured AC conductivity σ_{ac} consists of two parts, $\sigma_{ac} = \sigma_{dc} + A\omega^s$, where σ_{dc} is the frequency-independent DC component (due to inter-well hopping) and $A\omega^s$ is the frequency-dependent AC component (due to intra-well hopping) [26]. Here ω is the angular frequency of applied AC field and A and s are composition and temperature dependent parameters.

The hopping conduction increases with increase in the applied field frequency. The reason is that the grains become more active, thereby increasing the hopping probability of holes between the Ni^{3+} and Ni^{2+}ions. Thus, a gradual increase in conductivity with frequency is observed. At 303 K, the value of σ_{ac} is 0.03835 S/m at 100 Hz, which increases to 0.06047 S/m at 1 MHz. A slight decrease in the AC conductivity of NiO occurs, when CoPc is added to it, which may be due to trapping of charge carriers.

4 Conclusion

NiO/CoPc nanocomposite is synthesized by simple solvent evaporation method. The effect of frequency on the electrical properties of the composite at different temperatures is studied. The large value of ε' at low frequency is due to the space-charge polarization caused by impurities or crystal defects. The presence of two semicircular arcs in the Cole-Cole plot points out the existence of grain and grain boundary conduction in the nanocomposite sample. The variation of AC conductivity with frequency is explained based on correlated barrier hopping model. High dielectric constant together with good thermal stability makes the NiO/CoPc nanocomposite a promising material as embedded capacitors for decoupling applications and in the field of non-volatile memory.

The authors acknowledge nanoscience research centre (NSRC), Nirmala College, Muvattupuzha and Newman College, Thodupuzha, for providing the facilities to conduct this study. They are also grateful to SAIF Cochin and Maharajas College, Ernakulam, for the technical support rendered. The first author acknowledges UGC for facilitating the research work through FDP.

Author contribution statement

We, the authors, hereby inform that we all have contributed equally to this paper.

References

1. G.D. Wilk, R.M. Wallace, J.M. Anthony, J. Appl. Phys. **89**, 5243 (2001)
2. B.V. Prasad, G. Narsinga Rao, J.W. Chen, D. Suresh Babu, Mater. Res. Bull. **46**, 1670 (2011)
3. S. Saravanan, C. Joseph Mathai, M.R. Anantharaman, S. Venkatachalam, P.V. Prabhakaran, J. Appl. Polym. Sci. **91**, 2529 (2004)
4. T.D. Anthopoulos, T.S. Shafai, Appl. Phys. Lett. **82**, 1628 (2003)
5. M. Kaneko, T. Taneda, T. Tsukagawa, H. Kajii, Y. Ohmori, Jpn. J. Appl. Phys. **42**, 2523 (2003)
6. V. Biju, M.A. Khadar, Mater. Res. Bull. **36**, 21 (2001)
7. P.A. Sheena, K.P. Priyanka, N. Aloysius Sabu , B. Sabu, T. Varghese, Nanosystems **5,** 441 (2014)
8. A. Dias, R. LuizMoreive, J. Mater. Res. **12**, 2190 (1998)
9. H.S. Soliman, A.M.A. El-Barry, N.M. Khosifan, M.M. El Nahass, Eur. Phys. J. Appl. Phys. **37**, 1 (2007)
10. B.D. Cullity, *Elements of X-Ray Diffraction* (Addison-Wesley, Reading, MA, 1956)
11. K.V. Rao, A. Smakula, J. Appl. Phys. **36**, 2031 (1965)
12. C.G. Koops, Phys. Rev. **83**, 121 (1951)
13. K.W. Wagner, Am. Phys. **40**, 317 (1973)
14. P. Lunkenheimer, A. Loidl, C.R. Ottermann, K. Bange, Phys. Rev. B. **44**, 5927 (1991)
15. D.P Snowden, H. Saltzburg, Phys. Rev. Lett. **14**, 497 (1965)
16. R. Parker, D. Elewell, J. Appl. Phys. **17**, 1269 (1966)
17. K.K. Babitha, K.P. Priyanka, H. Hitha, S. Rintu Mary, E.M. Mohammed, S. Sankararaman, T. Varghese, J. Electron. Mater. **46**, 6234 (2017)
18. P. Mario Lanza, Materials **7**, 2155 (2014)
19. K.P. Priyanka, J. Sunny, T. Smitha, E.M. Mohammed, T. Varghese, J. Basic Appl. Phys. **2**, 105 (2010)
20. S.K. Aniban, A. Dutta, RSC Adv. **5**, 95736 (2015)
21. J. Xu, C.P. Wong, Compos. Part A Appl. Sci. Manuf. **38,** 13 (2007)
22. A.K. Thomas, K. Abraham, J. Thomas, K.V. Saban, J. Am. Ceram. Soc **5** (2017)
23. L.D. Sappia, M.R. Trujillo, I. Lorite, R.E. Madrid, M. Tirado, D. Comedi, P. Esquinazi, Mater. Sci. Eng. B. **200**, 124 (2015)
24. V. Varade, G.V. Honnavar, P. Anjaneyulu, K.P. Ramesh, R. Menon, J. Phys. D Appl. Phys. **46,** 365306 (2013)
25. M.R. Biswal, J. Nanda, N.C. Mishra, S. Anwar, A. Mishra, Adv. Mater. Lett. **5**, 513 (2014)
26. A.K. Jonscher, Nature **267**, 673 (1977)